

### **3. RESEARCH SUPPORT FACILITIES**

#### **3.1 HIGH VACUUM LABORATORY**

M. Archunan, A.Kothari, P.Barua and A. Mandal

During this academic year the HYRA beam line has been installed. With this all the beam lines of phase -II have been installed and beams have been delivered through them. Design and fabrication of vacuum interlocking system for diagnostic system in LINAC line was done and installed. Fabrication and installation of pneumatic valve controllers were completed at five new locations. Faraday cup at FC07-1 was replaced by a new flange mountable NEC Faraday cup.

Centralized purchasing of essential vacuum components from local and import is carried out regularly to maintain essential components in stock. Contaminated penning gauges are cleaned and tested regularly to maintain stock of gauges in working condition and for replacement. Regular involvement with the pelletron group in maintenance activities (scheduled and emergency) requiring vacuum operations, maintenance of vacuum pumps and installation of critical components was there.

##### **3.1.1 Phase - II Beamline Installations**

Installation of HYRA beamline : In continuation with the installation of beamlines in phase-II, the remaining HYRA beamline installation was completed at 40 degrees. Accurate alignment of Quadrapole, BPM and Faraday cup was done within 0.5 mm accuracy. Two beamline isolation valves, vacuum gauges and fast closing valve sensor, vacuum pumps like Ion Pump and Getter pump along with pumping cross were installed in the beamline. Beamline was properly baked and vacuum was established at around  $1 \times 10^{-9}$  Torr.

To test the beam in HYRA an arrangement was made to connect the beamline exit to HYRA experimental chamber. A drift tube, turbo pumping system, vacuum gauges and an additional BPM were installed and aligned for the beam test.

Fabrication and Installation of Beam line selector & Fast Valve interface: One Beam Line Selector for Phase - II has been designed, fabricated and Installed. The Fast valve Interfacing system was also designed, fabricated and installed in the same Box. Using this controller any one of the four Beam Lines in Phase - II can be selected during an experiment. And that particular Line will get interfaced with the Fast Closing Valve installed in Phase - II.

##### **3.1.2 Maintenance Activities**

Replacement of Material Science Beamline Valve: Vacuum valve (BLV L5-2) had a through leak and experiment could not be started because of bad vacuum. The valve installed was pneumatic straight through valve from NEC (NEC PSTV) and no further seat adjustment was possible. Because of repeated occurrence of such problems we replaced the valve with a DN 40 CFF VAT all metal valve on emergency basis.

Replacement of Fast Closing Valve BLV 02-1 in 02 Area: Fast Closing Valve BLV 02-1 of 02 area was showing leak and replacement of the valve was done. Ion source side vacuum was not holding better than  $1 \times 10^{-4}$  Torr so it was rectified by valve seat adjustment. The Buncher had a leak in the cooling coil because of which the vacuum of the region was not good for an year. The leak was detected and rectified.

### 3.1.3 Regeneration of Ion Pump using UHV set-up

An Ion Pump after continuous use for long time (3 - 4 years) in a decently managed vacuum system requires to be regenerated for its proper working. The main aim is to prepare the surface again before reusing the pump. UHV set up being used is equipped with a turbo pump backed by a dry pump, Residual Gas Analyser, an Ion pump, UV baking lamp and UHV Gauge of  $1 \times 10^{-11}$  mbar range. The system [Fig. 1] is maintained at around  $5 \times 10^{-10}$  mbar.

The process starts by removing the faulty anode assembly from the pump. It is mechanically cleaned to remove scales and deposits from the surface. The Ion pump is then electro polished from inside to make it perfectly clean. The surface brightens up after removal of micro irregularities from the surface. A new set of anode assembly is fitted in the pump. The Ion pump is then mounted on the testing side of the UHV setup. The pump is then baked at high temperature for a few days. When the background of the system matches with that of the clean environment the Ion pump is switched on and monitored. After the pump is ready, it is dismantled from the system and stored under vacuum for future use.

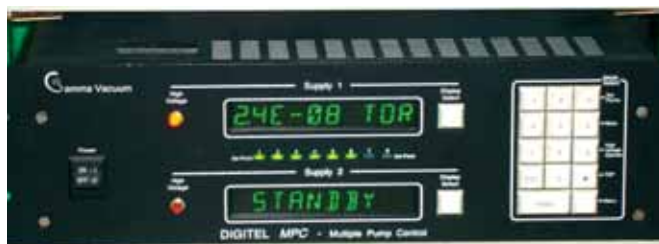


Fig 1. UHV set up

### 3.1.4 Development Work

Automatic power-on circuit for digital multiple controller (Ion pump controller ) is designed. The New Ion Pump controllers, after Power failure, goes to Standby Mode when the power resumes and have to be manually switched OFF and then switched ON again, for resetting the controller in Active Mode. A Circuit has been designed and tested to automatically do this job whenever this occurs. The circuit has been designed in such way that it will always monitor the ION Pump Controller. By this monitoring, it will automatically Switch OFF and then Switch ON the mains Input power of the Controller, if the controller goes to the Standby Mode. This is working fine and installation work is in progress.

### 3.1.5 Installation Work

#### **Installation of turbo pumping system for diagnostic system in LINAC beamline**

There is a Diagnostic System before the LINAC Cryostat. This system is being exposed in atmosphere frequently by the user. But it was not having any proper pumping system. Because of this, the required vacuum could not be established in this system as well as in the LINAC beam line. So one Turbo pumping system with Isolation valve, vent valve, Pirani Gauge, Dry Scroll pump and two pneumatic valve (for backing) have been installed for this Diagnostic System. A new vacuum interlock specific for this system was designed, fabricated and installed.

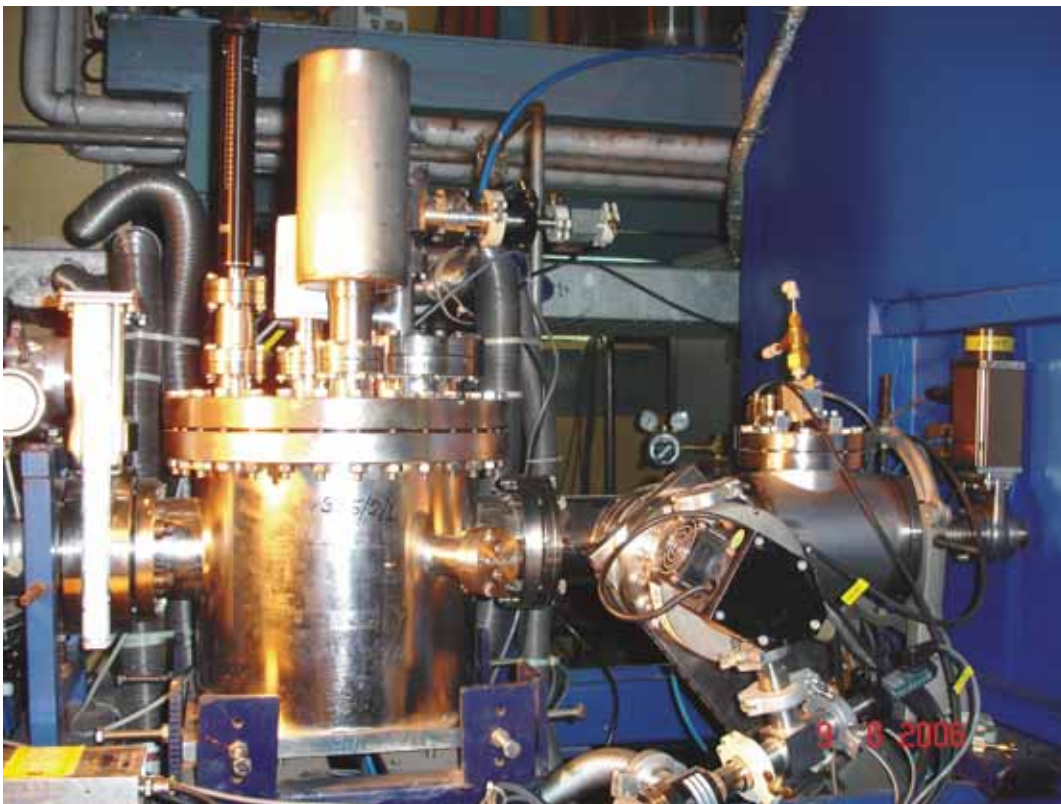


**Fig. 2 Turbo Pumping system at Diagnostic Box LINAC**

### 3.2 MAINTENANCE OF MAGNETS AND POWER SUPPLIES

S.K.Suman, Rajesh Kumar, A.J.Malayadri and A.Mandal

Beam transport group has been performing regular maintenance of magnets, power supplies, their CAMAC Modules, different types of magnetic field measuring instruments, magnet selector switchgear etc. to keep uptime of beam transport system maximum. There are different types of magnets in our systems which are powered by highly stable power supplies. To keep the performance of BTS devices better, we have done the following major jobs in this year.

**Routine Maintenance:** Routine maintenance of all magnets and their power supplies are done twice in a year where following scheduled tasks are carried out:

- Stability measurement and rectification of bending magnet power supplies.
- Output ripple monitoring of all power supplies and rectification, if any.
- Interlock testing of all magnet power supplies.
- Readback calibration of all magnet power supplies.
- Dust cleaning of electronic cards of all magnet power supplies.
- Through observation of all power devices like power contactors, power transistors and water cooled heatsinks etc and changing faulty devices.
- Checking input and output power connections for loose contacts.
- Changing damaged hose pipes.
- Temperature monitoring of all magnets at rated capacity to observe its cooling efficiency and cleaning the partially blocked coils with high pressure water or sulphamic acid.

This year, following major repair jobs have been done:

- Water cooled heatsinks of PH-I bending magnets and quadrupole magnets were replaced by new ones. The water leaking because of corrosion of existing heatsink could be eliminated.
- Rubber hose pipes were replaced with silicon ones inside water cooled power supplies to minimise the hose pipe bursting due to high pressure water.
- Vario transformer of analyser magnet power supply was overhauled. Sliding mechanism was not working properly and a few current collecting plates/ bars, carbon wheel were faulty. All sliding parts have been cleaned, realigned and the damaged parts have been repaired.

**Breakdown maintenance:** No major breakdown occurred this year. All magnets, power supplies performed well.

### 3.3 DETECTOR LABORATORY

A. Jhingan, P. Sugathan and R. K. Bhowmik

Detector Laboratory at IUAC provides experimental support to various users in setting up charged particle detectors and readout electronics. New detectors and electronics have been designed and developed for new experimental facilities. Apart from various developmental activities, the group is intensively involved in various user experiments in nuclear reaction dynamics in HIRA, GPSC and Neutron Array using heavy ion beams. Detector lab provided special training on experimental activities for Scientist Trainees, JRF students, and M.Sc orientation program students.

#### 3.3.1 Large area position sensitive annular PPAC

A. Jhingan, T. Varughese, Sugathan. P, R. K. Bhowmik and H. J. Wollersheim\*

A large area Annular PPAC development was taken up last year. The detector setup will be used in GDA for Coulomb excitation experiment. The detector has been designed and fabricated with two electrode geometry. Two sets of electrodes with different active areas were designed and fabricated using commercially available 2.4mm thick G-10 PCB.

The cathode plane is segmented into 16 parts to provide angle information in phi plane at 22.5 degree resolution. The foil was stretched and pasted on a commercially available custom designed 2.4mm thick G-10 PCB. The anode plane is made of 2.4mm thick PCB which has concentric rings segmented into two halves. The rings are interconnected by delay line chips placed on the rear side. Thickness of each ring is about 2.5 mm. The fabrication process of the annular PPAC is expected to be completed by end of May. Installation of detector in GDA beam line will be done around September and the Coulomb excitation experiments are likely to be carried out in November 2007.

\* GSI, Germany

#### 3.3.2 CsI + PIN photo-diode detector for particle identification

CsI based charged particle detector was tested offline for pulse shape discrimination properties using standard zero-cross technique and ballistic deficit technique for particle identification. The CsI crystal used (Manufactured by Scionix, Holland) has an active area of 50mm x 50mm x 10mm tapered to a 18mm x 18mm Hamamatsu photo diode. A home made low noise charge sensitive pre-amplifier was mounted right next to the photo diode to minimize the noise and loss of signal in coaxial cable. The whole assembly is mounted inside an Aluminum box.

The detector was tested with different radioactive sources such as Cs<sup>134</sup>, Cs<sup>137</sup>, Co<sup>60</sup>, Am<sup>241</sup> and Cf<sup>252</sup>. To study the PSD properties and for charge particle detection, entire setup was placed inside the detector lab vacuum chamber. Ballistic deficit and Zero cross techniques were tried simultaneously. Good discrimination was observed between gammas (from CsI crystal), alphas, and gammas (directly from PIN diode) using both the techniques as shown in the fig. 1. For Zero cross technique a tripolar shaped pulse was generated, by combining two bipolar signals of 0.5 us and 1us time constant, to generate the start for TAC. This was required since rise times of

CsI are very slow and thus generating a CFD trigger by conventional techniques is very difficult. Off line proton generation was also attempted using Rutherford scattering of alphas (from Am<sup>241</sup> and Cf<sup>252</sup>) with polypropylene foil. Statistics and energy of observed protons were too low to confirm detection of protons in CsI. It is planned to carry out beam tests with Pelletron to study proton-alpha-gamma discrimination.

### 3.3.3 Charge sensitive Pre -Amplifiers

Vacuum compatible charge sensitive preamplifiers developed by detector lab were used with high capacitance cooled silicon surface barrier detectors in a GPSC experiment (Dr. A. Ray : VECC, Kolkata) with Pelletron (19F + 27Al). The preamplifiers were used with TOF systems consisting of 5 micron thick, 50 mm<sup>2</sup> area (detector capacitance ~ 1000pF) and 8.6 micron thick

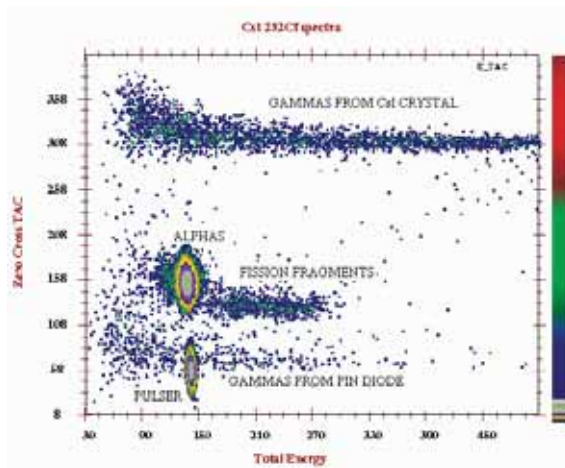


Fig.1a: Zero cross PSD spectrum

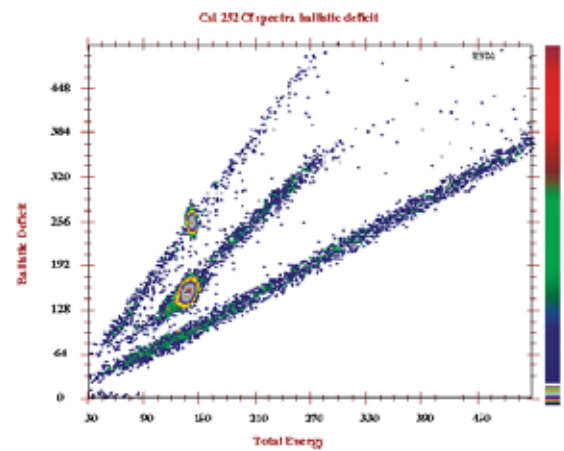


Fig.1b: Ballistic deficit PSD

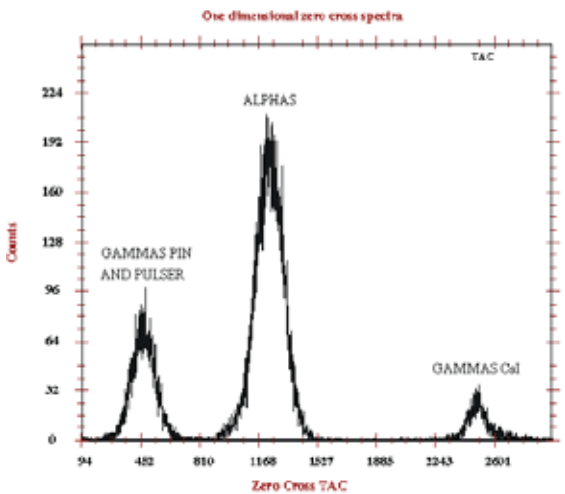


Fig.1c: Zero Cross 1D projection

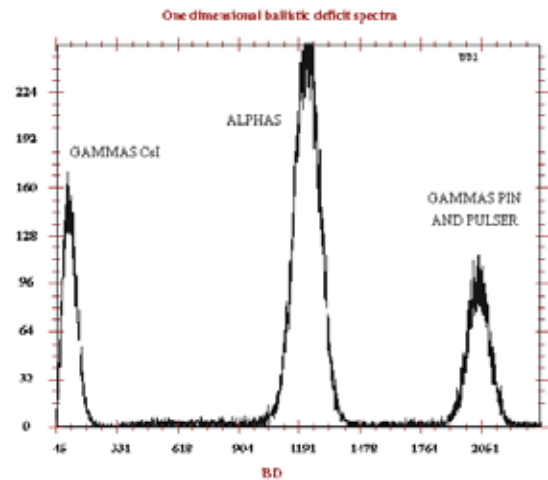
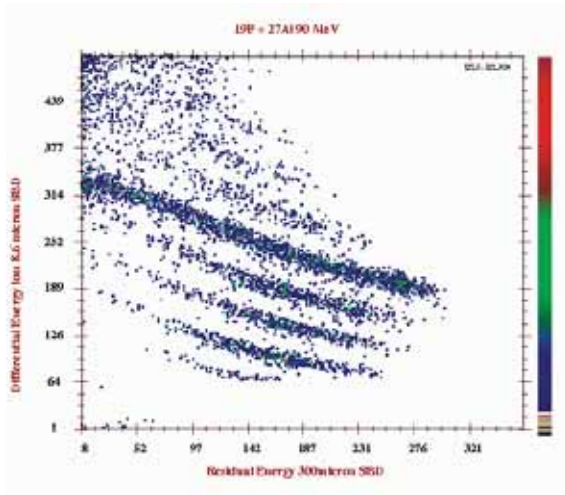


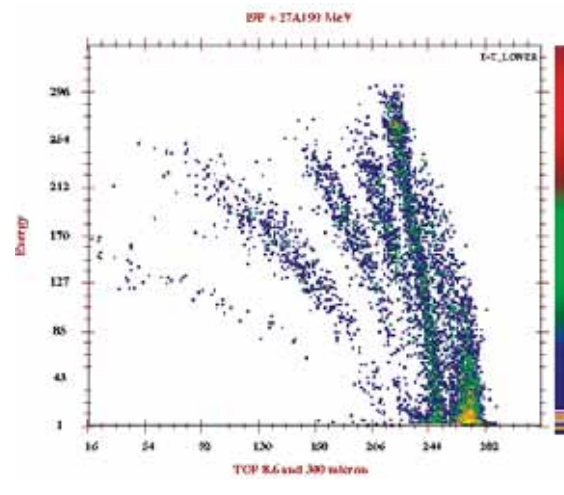
Fig.1d: Ballistic deficit 1D projection

Fig.1. PSD spectrums from CsI crystal coupled to photodiode

50 mm<sup>2</sup> area (detector capacitance ~ 600pF) surface barrier detectors as start detectors and 300 micron thick, 200mm<sup>2</sup> area SBD as stop detectors. Good energy and TOF resolutions were observed which was compatible with Canberra 2003BT preamplifier put on separate TOF system in the experiment. The main aim of the experiment is to do isotope identification (oxygen isotopes). Fig.2 shows the spectrums taken from TOF system comprising 8.6 and 300 micron SBD placed 40 cm apart. Modifications in the preamp timing output are being explored to improve TOF resolution which is essential for isotope identification.



**Fig.2a : dE-E spectrum**



**Fig.2b : TOF spectrum**

**Fig.2. Particle identification spectrums using dE-E and TOF techniques**

### 3.3.4 MWPC for Neutron Array

A.Jhingan, T. Varughese and P.Sugathan

Two new position sensitive multiwire proportional counters have been designed and are currently under fabrication for use in neutron array chamber. The detectors will be used for detecting complementary fission fragments. The detectors will have a three electrode geometry having a cathode frame sandwiched between two position frames giving X and Y positions. The electrodes will be housed inside a rectangular aluminium chambers milled from solid aluminium block. Detectors will have an active area of 125mm x 75mm. Positions will be derived using delay line chips and are expected to give a position resolution of 2mm. To improve the avalanche capabilities and thus timing resolutions at low pressures, it is planned to use 10 micron gold plated tungsten wires against 20 micron and reduce the wire pitch to 0.6mm against 1.27mm as used in previous MWPCs for position electrodes, and aluminised mylar for cathode. Fabrication of detectors is expected to be completed by April end.

### 3.3.5 Neutron-gamma discrimination using QDC

A. Jhingan, Hardev Singh, R. P. Singh, K. S. Golda, P. Sugathan, R. K. Bhowmik

Neutron gamma discrimination was performed using digital charge comparison technique with commercially available Phillips CAMAC charge to digital converter. A 5" x 5" BC501 Bicron liquid scintillator coupled to Phillips XP4512B PMT was exposed to Am-Be and <sup>252</sup>Cf neutron sources. The signal from the PMT anode is transmitted through RG58 coaxial BNC cable of about 50m length to the data room from beam hall I. The signal is thereafter split into 3 parts using an active splitter. Active splitter is required since passive splitter while driving simultaneously to three 50 ohm loads, namely CFD and two QDCs each of which has a 50 ohm input impedance, leads to massive attenuation and distortion of anode pulse which is not acceptable in our kind of application. The outputs of the CFD is fed to gate and delay generator which generates the respective gates for integrating the fractional charge, total charge as well as the master gate. As shown in the fig. 3, good n-g discrimination is observed with thresholds as low as 130 keV which corresponds to 400 keV protons. The data in the figure is taken with 100mC Am-Be source at count rate of 10kHz. FOM observed is about 1.3. Fig.2a is the 2D plot between fractional charge (Y-axis) and total charge (X-axis), and fig.2b is the 1D normalised PSD projection. A NIM module has been developed which houses 6 channels of active splitter along with passive analog delays. Analog delay is required to delay the PMT anode signal to be integrated by QDC.

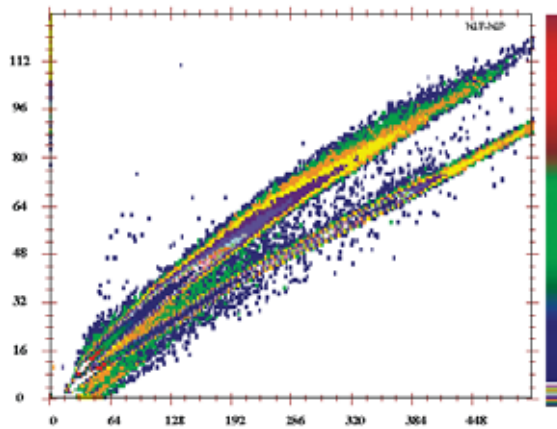


Fig. 3a

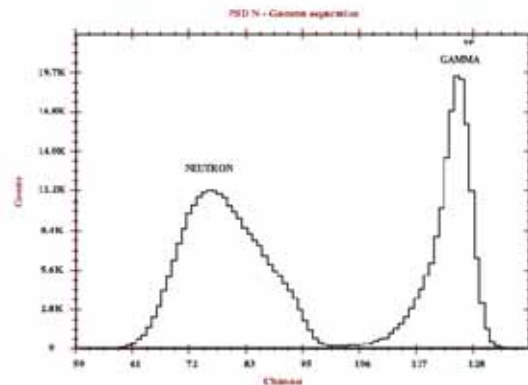


Fig. 3b

Fig.3. PSD spectrum of BC501 liquid scintillator on exposure to Pu-Be source

### 3.3.6 New HIRA Focal Plane Detector system

A. Jhingan, P. Sugathan, Ranjeet Dalal, T. Varughese, Hardev Singh, J. Gehlot, S. Nath, J. J. Das, N. Madhavan, R. P. Singh, P. Shidling<sup>1</sup>, B. R. Behera<sup>2</sup>, S. K. Mandal<sup>3</sup>

<sup>1</sup>Dept. of Physics, Karnataka University

<sup>2</sup>Dept. of Physics, Punjab University

<sup>3</sup>Dept. of Physics, Delhi University

A new detector system consisting of a large area, transmission type, two dimensional position sensitive MWPC (fig.4) followed by a compact deep gas ionization chamber (IC) was

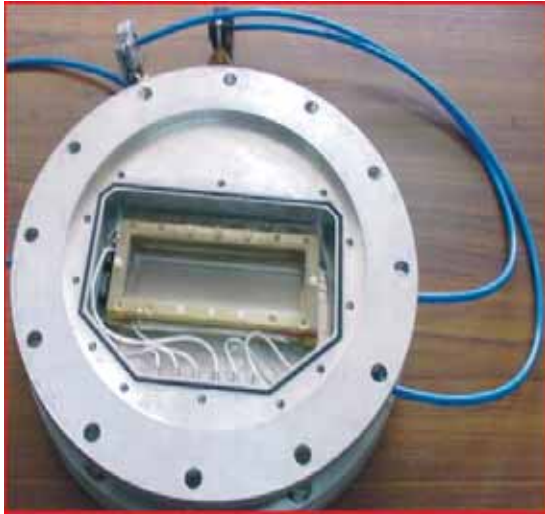


**Fig.4. MWPC**

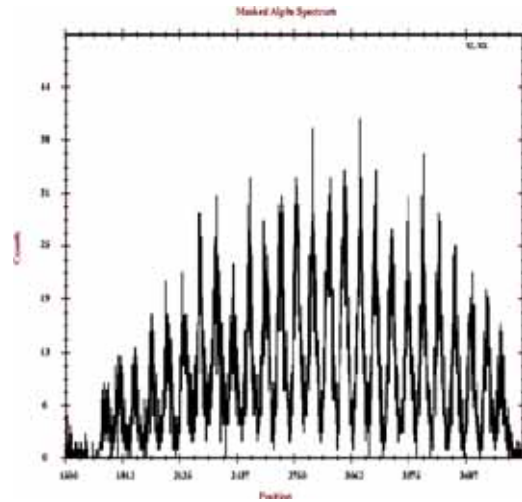


**Fig.5. Masked alpha spectrum from X - position**



**Fig.6. IC electrode assembly**



**Fig.7. IC & MWPC at HIRA focal plane**

installed at HIRA focal plane as shown in fig.7. The detector was tested offline with  $^{241}\text{Am}$  alpha source, and used online in the experiment (as described later in the report).

The MWPC has an active area of 6" x 2" and has a 5 electrode geometry namely two cathodes (giving energy loss in active area) sandwiching two position electrodes (giving X and Y coordinates of the particles reaching focal plane using delay line timing technique) and a central anode (giving timing information for TOF and positions). All electrodes are made up of 20 micron diameter gold plated tungsten wires at 1.27mm pitch, and are placed 3.2mm apart. Entire electrode assembly is mounted inside a cylindrical aluminum chamber milled from solid aluminum block as shown in the fig. The MWPC was tested offline with alpha source at 3mbar isobutane. MWPC is isolated from focal plane vacuum (low  $10^{-8}$  Torr) using 1 micron thick mylar foil. Fig.5 shows a masked position spectrum. The mask has 1mm diameter hole placed 5mm apart. Source to mask distance is about 20cm and mask to detector distance is 5cm. A position resolution of about 2mm FWHM has been observed. The detector was operated at 1.5mbar isobutane for inbeam experiment  $^{40}\text{Ca} + ^{68,70}\text{Zn}$ . The detector could handle count rates exceeding 100kHz without any breakdown. Inhouse developed fast timing current preamp was used for anode readout. The signal had a rise time of better than 10ns with good signal to noise ratio. Mass information of fusion products and its separation from beam like particles was performed using X-position signal, TOF (from anode) w.r.t. RF (pulsed beam from pelletron), and the energy loss signal given by cathode.

The IC, as shown in fig.6, is of transverse field geometry type having segmented anode (three segments in longitudinal direction w.r.t. beam) for particle identification, frisch grid placed 1cm apart from anode, and a cathode placed 5cm from frisch grid. The design is inspired by IC developed by Daresbury Laboratory in early eighties. The detector was operated at 10-60 mbar isobutane during in beam beam experiment ( $^{40}\text{Ca} + ^{68,70}\text{Zn}$ ), and at 100 mbar for offline alpha test. The IC is isolated from MWPC by a 1 micron thick mylar foil of active window area 7cm x 3cm. Fig.8 shows the spectrums taken from exposing detector to Pu-Am mixed alpha source and transfer reaction products of  $^{40}\text{Ca} + ^{70}\text{Zn}$ . The total energy resolution obtained by summing gain matched signals of second and third segment (fig. 8C) is about 3.5 % fwhm (for Am241) for about 4.2 MeV energy deposition. Remaining energy is lost in entrance mylar windows, MWPC, dead regions and first segment of IC. Inferior energy resolution is observed for the first segment which is due to its small length (~3cm) and thus smaller energy deposition, and non uniform charge collection due to bulging of entrance window foil because of high gas pressure. An additional guard electrode will be added in coming days on the entrance side to improve the resolution of the first segment. We would like to acknowledge the support from Mechanical Workshop (IUAC) and Vacuum Lab (IUAC) for their invaluable support during installation and operation of the new detector system.

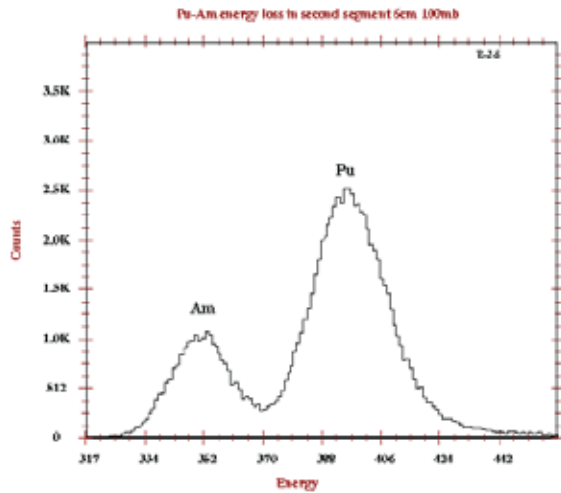


Fig.8A. Energy loss in 2nd segment

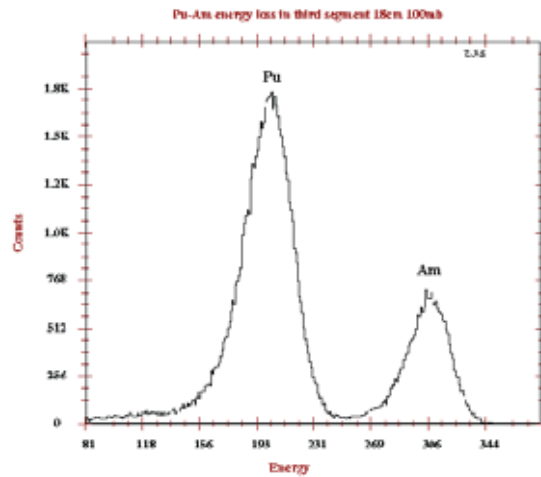


Fig.8B. Energy loss in 3rd segment

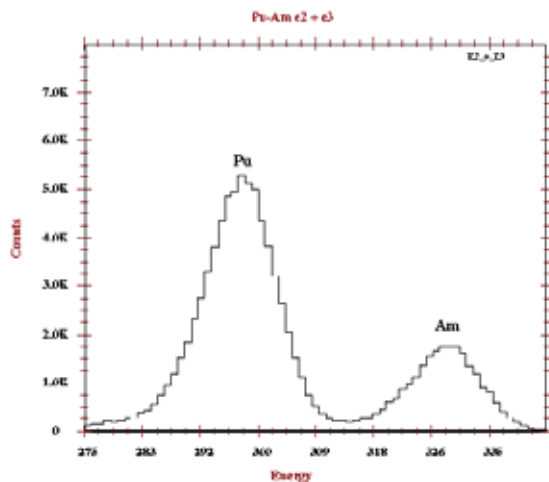


Fig.8C. Total energy (E2 + E3)

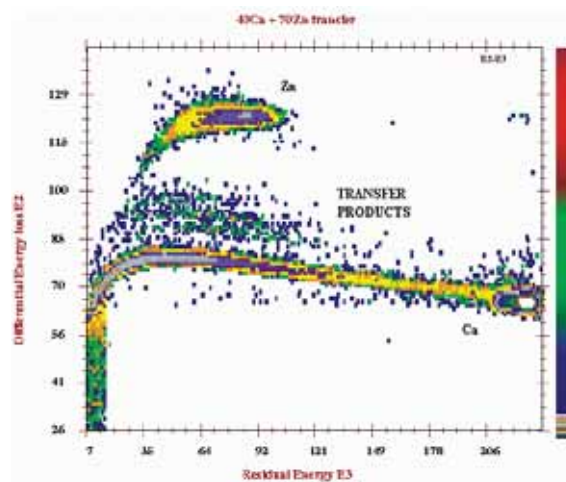


Fig.8D. E2 vs E3 for  $^{40}\text{Ca}+^{70}\text{Zn}$

Fig.8. Spectrums obtained from ionization chamber

### 3.3.7 Large area MWPCs of GPSC

The two large area MWPCs (8" x 4") have performed well since 2004 July and have been actively used in GPSC (beam hall I) and Neutron array chamber (beam hall II) experiments for detecting fission fragments. No leakage in pressure foils (mylar window 1 micron thick) have been observed. In September 2006, one of the MWPCs had its one cathode wire frame damaged, as a result of which it was not taking bias. The faulty wire frame will be replaced very soon and used in forthcoming fission experiments in GPSC.



**Fig.9A. Entrance view of MWPC**



**Fig.9B. MWPCs mounted in GPSC**

**Fig.9. Large area MWPC for GPSC**

### **3.3.8 Operation of MWPC with Helium gas**

A. Jhingan, P. Sugathan, A. Roy and R. K. Bhowmik

Operation of MWPC (described in section 3.3.6) using low pressure Helium gas was attempted. At 2 mbar pressure breakdown was taking place at low voltages ( $< 150\text{V}$ ) and no signal could be seen. The Helium gas was then mixed with some isobutane (10 - 20 %), which acts like a quencher, and fairly good signals could be seen when detector was exposed to Am241 alpha source. Quality of timing signal (from anode and delay line position electrodes) and breakdown voltage is dependent on the concentration of isobutane gas mixed with Helium whereas the actual amplitude of the energy signal from cathode is dependent on the the concentration of Helium gas. The delay line chips used in MWPC have a 50 ohm impedance are bandwidth limited and thus position signals were found to be very weak with poor S/N ratio. The situation will be better with heavy ions. Alternatively high impedance delay line chips will be tried in future to improve the position signal quality. The main idea of operating MWPC with Helium gas is to use it in HYRA without pressure mylar foil. HYRA in its gas filled mode will be operated with low pressure Helium gas at low pressures (1~2 Torr). Low velocity heavy residues formed in fusion reactions suffer heavy attenuation and straggling even in very thin mylar foil (~1 micron). Elimination of mylar foil will facilitate detection from large area MWPC which in contrast to large area Silicon detectors can handle larger count rates, without radiation damage, and provide better timing resolutions with larger active areas. Differential pumping is planned to avoid total contamination of Helium gas with isobutane in the active region of gas filled magnets. In coming days, operation of MWPC at lower pressures ( $< 1\text{ Torr}$ ) will be attempted with different concentrations of isobutane (5 -20 %). For precise pressure control digital gauges will be used. Attempts are also on for fabricating custom electronics for high impedance delay line. Some preliminary designing has already been worked out.

### 3.3.9 Tracking detector systems for RMS focal plane

J. J. Das, A. Jhingan, P. Sugathan and R. K. Bhowmik

Tracking detector systems comprising of position sensitive MWPCs, IC and transmission ICs are planned for charged particle detection at HIRA/HYRA focal planes. The detector systems will work as TOF system, particle identification system, and will be used for ray tracing to determine the trajectory of the particle. Two different kind of systems are planned for HIRA and HYRA respectively. Some preliminary designs have been worked out along with readout electronics. Currently ion optic simulations are being carried out for detector system. In coming days some preliminary measurements will be performed with the existing detector systems to explore the feasibility on improving detector designs and its readout electronics. Fig. 10 shows the tentative design of tracking detector for HYRA focal plane.

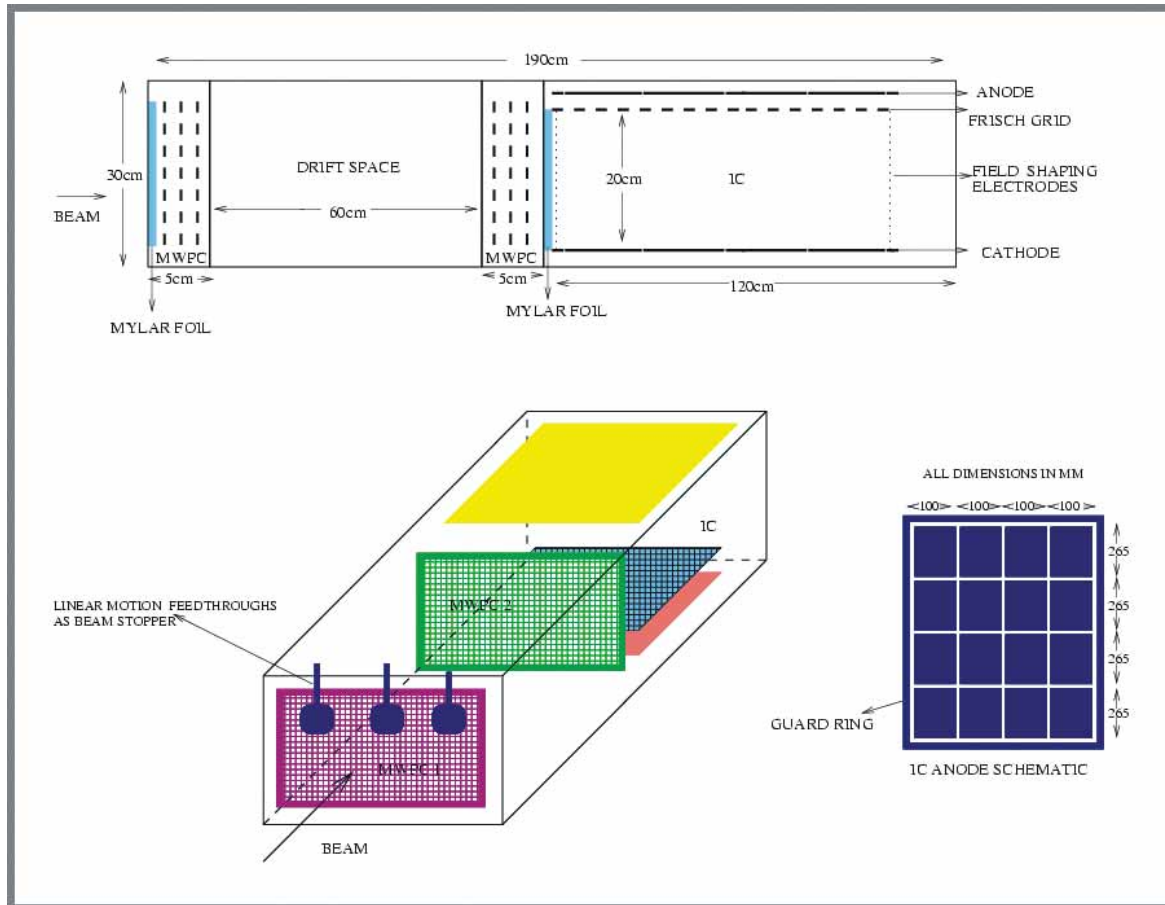


**Fig.10. Tentative schematic of tracking detector for HYRA focal plane**

### 3.4 TARGET DEVELOPMENT LABORATORY

D. Kabiraj, Abhilash S. R and D. K. Avasthi

Target Development Laboratory at NSC provides facilities to the users for the preparation of targets used for the experiments with NSC Pelletron. The laboratory has the following facilities: (i) a high vacuum evaporator, equipped with 2kW electron beam gun, evaporation setup by resistive heating, online thickness monitoring by quartz crystal thickness monitor. This evaporator is pumped by a diffusion pump with liquid nitrogen trap, with a base pressure of high  $5 \times 10^{-7}$  mbar. (ii) The oil free pumping system for the second evaporator includes a cryo-pump, a turbo molecular pump and a scroll pump, with a base pressure of  $6 \times 10^{-9}$  mbar. This evaporator is equipped with a 6kW 4-pocket electron gun and evaporation setup by resistive heating method and a dual crystal thickness monitor and controller for online thickness monitoring and process control. (iii) A rolling machine for the preparation of thin foils by cold rolling method.

More than 70 users have used this facility for the preparation of thin films for their studies in the areas of Nuclear Physics, Atomic Physics and Materials Science. There were several thin films prepared in this year which includes 600 carbon stripper foils of less than  $5 \text{ mg/cm}^2$  thick used for NSC Pelletron. Some of the interesting and important thin films prepared this year are mentioned later.

Highly transparent, conducting, highly oriented, and almost single phase ZnO films have been deposited by simple e-beam evaporation method, and the deposition parameters were optimized [1]. The films were prepared by (a) evaporation of ZnO at different substrate temperatures and (b) evaporation of ZnO at room temperature and subsequent annealing of the films in oxygen ambient at different temperatures. The characterizations of the film were performed by optical absorption spectroscopy (UV-visible), Fourier transform infrared spectroscopy, resistivity measurement, transmission electron microscopy (TEM), photoluminescence, and x-ray diffraction measurement. Absorption spectra revealed that the films were highly transparent and the band gap of the pre- and postannealed films was in good agreement with the reported values. The band gap of the films increases on increasing the substrate temperature as well as annealing temperature, whereas the resistivity of the film decreases with substrate temperature and increases with annealing temperature. Fourier transform infrared spectroscopy of ZnO films confirms the presence of Zn-O bonding. X-ray diffraction, electron diffraction, and TEM images with high resolution and Raman spectra of the films showed the formation of crystalline ZnO having wurtzite structure.

Charge retention properties of Ge nanoparticles embedded in  $\text{SiO}_2$  matrix have been studied. Formation of embedded Ge nanoparticles was accomplished by electron beam evaporation in ultra high vacuum (UHV) conditions. Size of Ge nanoparticles has been characterized by atomic force microscopy (AFM) and the measured size was  $\sim 15 \text{ nm}$ . The size is smaller than the Bohr exciton radius ( $\sim 25 \text{ nm}$ ) for Ge nanoparticles. Capacitance-Voltage (CV) characteristics of the metal oxide semiconductor (MOS) structure shows the hysteresis of  $\sim 3.57 \text{ V}$  which gives the evidence of memory effect of Ge nanoparticles. (Y. Batra et al.)

The effects of room-temperature irradiation of Au and Ge nanoislands grown on Si have been investigated [2]. The samples were prepared using an UHV e-beam evaporation technique with a base pressure of  $5 \times 10^{-8}$  mbar. Au and Ge layers (each having 1 nm of nominal thickness as indicated by a digital thickness monitor) were evaporated on a native oxide covered Si(100) substrate using a deposition rate of  $0.01 \text{ nm s}^{-1}$ . The study shows the formation of Au-Ge alloy phase within the islands and wetting of the substrate. High-resolution transmission electron microscopy along with synchrotron radiation-based x-ray reflectivity and grazing incidence x-ray diffraction measurements were performed to characterize the irradiation-induced changes brought into the sequentially deposited Au and Ge island thin films. The results are attributed to the recoil implantation and the transient melting of the nanoislands followed by the formation of crystalline alloy phase.

Conducting nanowires parallel to each other, embedded in fullerene matrix are synthesized by high energy heavy ion irradiation of thin fullerene film at low fluence (up to  $5 \times 10^{11}$  ions/cm<sup>2</sup>) [3]. Fullerene thin films of 200 nm thicknesses were deposited on 50 nm thick Au layers on Si wafers. The need of Au layer was to facilitate the characterization of conducting channels by conducting atomic force microscope (C-AFM). First, 50 nm Au films were deposited on silicon substrate by resistive heating. Subsequently, the fullerene films were deposited on these Au films by sublimation of C60 pellet. The conductivity of the conducting zone is about seven orders of magnitude higher than that of the fullerene matrix. The conducting nanowires are evidenced by conducting atomic force microscopy. The typical diameter of the conducting tracks is observed to be about 40-100 nm. The creation of conducting wires is explained by transformation of fullerene to conducting form of carbon in the ion track, surrounded by the polymerized zone. The polymerization of fullerene is evidenced by Fourier transform infrared spectroscopy.

Several composite thin films of dielectric materials like oxides and polymers embedded with (i) noble metal, (ii) ferromagnetic metal nano-particles and (iii) semiconductor nano-particles have been prepared using indigenously built atom beam sputtering setup [4]. It is also used effectively for the purpose of nano-structuring of single crystal semiconductor surface through ripple formation [5]. The atom beam sputtering has certain advantages over conventional RF magnetron sputtering for the preparation of composite thin films. A saddle filed type, wide beam gun that delivers energetic neutral beam of Ar with energy ranging from 0.8 to 1.5 keV from MECA2000 (part of a DST funded project) has been used. For the fabrication of nano-composite thin films, a circular disc of the dielectric material is used as target. Small pieces of metal foils are glued on this surface. The area to be covered by the metal foil is determined by the metal fraction to be present in the matrix. Various aspects of these nano-composite thin films have been studied. The optical properties (surface plasmon resonance absorption) of Ag and Au nano-particle embedded oxide and polymer dielectric materials [6, 7, 8] and optical properties (photoluminescence, Raman) of Ge nano-particles in SiO<sub>2</sub> matrix [9] have been studied.

## REFERENCES

- [1] D. C. Aggarwal et al. J. Appl. Phys. 99 (2006) 123105.
- [2] T. Som. et al., Nanotechnology, 17 (2006) 5248.
- [3] Amit Kumar et al., J. Appl. Phys. 101 (2007) 014308.
- [4] D. Kabiraj et al., Nucl. Instr. Meth. B 244 ( 2006) 100.
- [5] P.K. Kulriya et al., Nucl. Instr. Meth. B 244 ( 2006) 95.
- [6] Y.K. Mishra et al., Scripta Materialia 56 (2007) 629.
- [7] D.K. Avasthi et al., Nanotechnology 18 (2007)125604.
- [8] Y.K. Mishra et al., Appl. Phys. Lett. 90 (2007) 073110.
- [9] A Singha et al., Semicond. Sci. Technol. 21 (2006) 1691.

### 3.4.1 Isotopic Tellurium target preparation by vacuum deposition

Anukul Dhal<sup>1</sup>, Rishi Kumar Sinha<sup>1</sup>, Abhilash S R<sup>2</sup>, and D Kabiraj<sup>2</sup>

<sup>1</sup>Department of Physics, Banaras Hindu University, Varanasi-221005

<sup>2</sup>Target Laboratory, Inter University Accelerator Centre, New Delhi-110067

Tellurium is a transition element which is not expected to behave like ductile metal and hence very thin self-supporting layers may be extremely difficult to obtain. As reported by [1, 2], tellurium targets are considered unstable in charged particle beams and the instability is often associated with thermal effects. Foils consisting of 1.13 mg/cm<sup>2</sup> of <sup>124</sup>Te deposited on aluminium backing of thickness 2.25 mg/cm<sup>2</sup> have been prepared. The targets were used in 1-2 pA beams of 150 MeV <sup>20</sup>Ne ion at Variable Energy Cyclotron Centre, Kolkata, India for the studies of <sup>144</sup>Sm compound nucleus at high spin by the reaction <sup>124</sup>Te+<sup>20</sup>Ne. Earlier works on Te targets [1, 3] describe the successful preparation of targets with thickness up to 1 mg/cm<sup>2</sup> upon gold backing. For our choice of beam and beam energy, it was well known from earlier experiments that Al backing is a good candidate, thus Al backing has been chosen for this target. Backing foils were prepared by sandwich rolling technique with the help of a rolling machine. S.S-304 plates of 0.75mm thick were used to roll the Al foils. The target fabrication was performed by resistive heating method using 55 mg of <sup>124</sup>Te as the source material with a source-to-substrate distance 4.5 cm. For the purpose of evaporation a special kind of evaporation source was used which was a tantalum tube having a narrow hole, of 1 mm diameter, in its center. After placing required amount of material both ends of the tube was closed by using a crimping tool. The reason for using such boat was: a) isotopic tellurium is very expensive and hence for utilizing minimum amount of material by increasing the collection efficiency. b) Powdered tellurium has a tendency to jump out of the open boat source. Figure 1 shows the schematic representation of the evaporation setup.

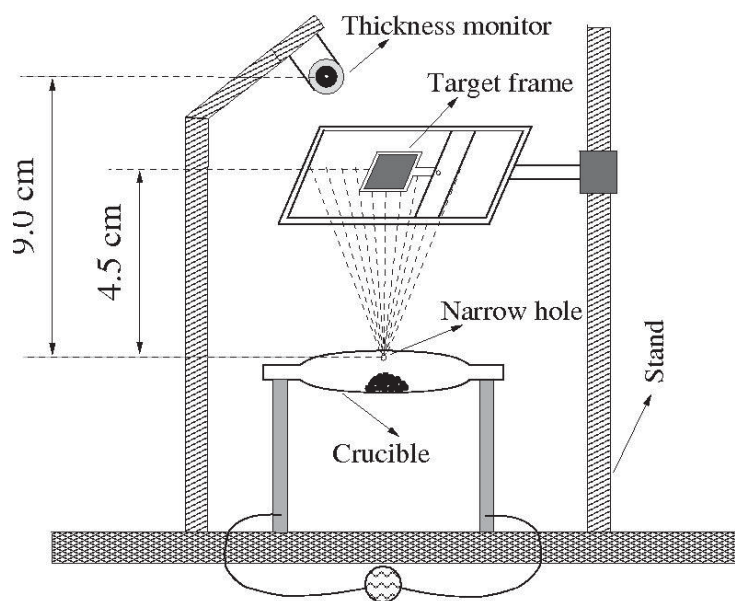


**Fig. 1. The schematic representation of the evaporation setup.**

## REFERENCES

- [1] G. Sletten, G.B. Hagemann, Nucl. Instr. and Meth. A 236, 647 (1985).
- [2] Anna Stolarz, Nucl. Instr. and Meth. A 438, 48 (1999).
- [3] J.P. Greene, G.E. Thomas, Nucl. Instr. and Meth. A 282, 71 (1989).  
(Presented at the DAE symposium on Nuclear Physics 2006)

### 3.4.2 Fabrication of $^{184}\text{W}$ target on carbon backing

P. D. Shidling<sup>1</sup>, Abhilash S. R.<sup>2</sup>, D. Kabiraj<sup>2</sup>, N. Madhavan<sup>2</sup>

<sup>1</sup>Department of Physics Karnatak University, Dharwad-580003

<sup>2</sup>Inter University Accelerator Centre, New Delhi-110067

Tungsten is a very hard material with high melting point (3387°C). It is difficult to prepare its thin film on carbon backing. The strain developed due to deposited tungsten layer ruptures the free standing carbon backing foils. With much effort using only 130mg of isotopically enriched  $^{184}\text{W}$  target of 200 mg/cm<sup>2</sup> were prepared on 100 mg/cm<sup>2</sup> of carbon backing. This target has been successfully used in two reaction experiments performed at IUAC. Several methods were adopted to convert the tungsten powder to a special pellet form to minimize the consumption of the expensive material, preparation of stress relieved carbon backing foil, steps taken to make the carbon withstand the heat generated during the tungsten evaporation. Experimental setup for tungsten deposition is shown in Figure 2.

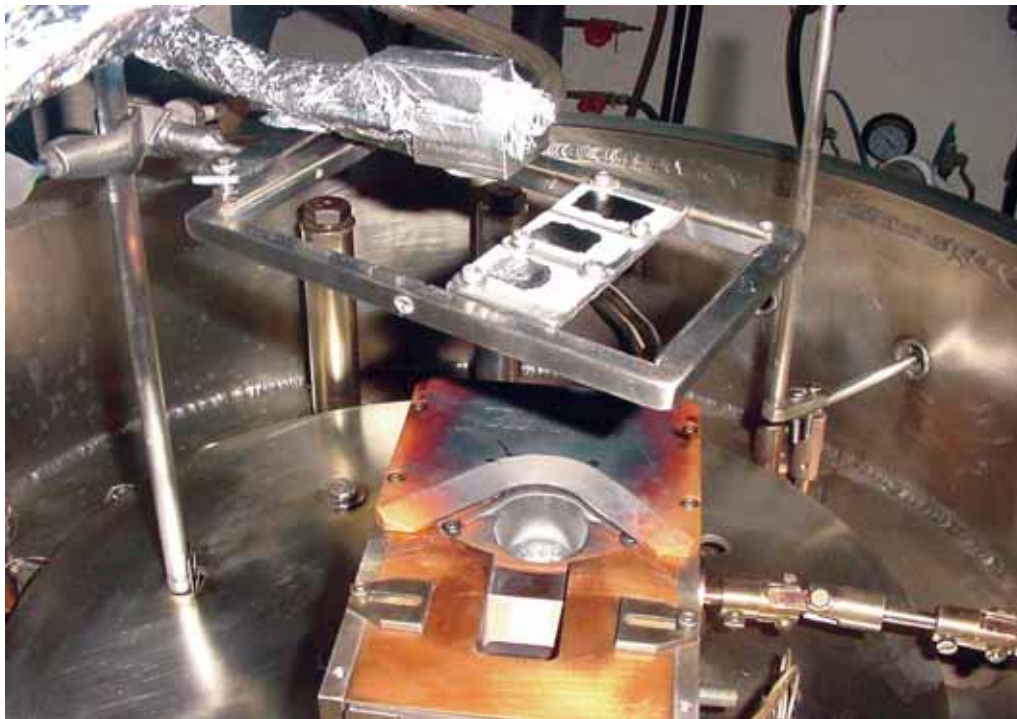


**Fig. 2. Experimental setup for tungsten deposition**

(Presented in the conference of International Nuclear Target Development Society 2006, held at Tsukuba, Japan)

### **3.4.3 Preparation of $^{181}\text{Ta}$ target by physical evaporation method**

P. D. Shidling<sup>1</sup>, Abhilash S. R.<sup>2</sup>, D. Kabiraj<sup>2</sup>, D. Mehta<sup>3</sup>, N. Madhavan<sup>2</sup>

<sup>1</sup>Department of Physics Karnatak University, Dharwad-580003

<sup>2</sup>Inter University Accelerator Centre, New Delhi-110067

<sup>3</sup>Department of Physics, Punjab University, Chandigarh

$^{181}\text{Ta}$  target has been prepared by vacuum evaporation method at the target development laboratory in IUAC, New Delhi.  $^{181}\text{Ta}$  were prepared both self-supporting and also on  $25\text{mg}/\text{cm}^2$  thick carbon backing foils. These targets are to be used in fission hindrance studies utilizing Heavy Ion Reaction Analyzer (HIRA) facility at IUAC.

For the preparation of self-supported tantalum target tantalum was evaporated on a rolled copper foil of thickness  $1.5\text{ mg}/\text{cm}^2$ . The rolled copper foil was mounted on the substrate heater as shown in Fig.3. The substrate was heated and maintained at a temperature  $3000\text{ }^\circ\text{C}$  during evaporation. The copper backing was chemically etched to obtain free-standing Ta foils as shown in figure 4.



**Fig. 3. Copper mounted on substrate heater**

XRF measurement was carried out to make sure about the absence of copper contamination in the tantalum target. XRF measurements were carried out at Punjab University, Chandigarh, using energy dispersive X-ray fluorescence spectrometer using X-ray tube. Measurements were carried out for two samples. Peaks at 8.1 keV, 9.3 keV and 11.8 keV were seen and these were tantalum La, Lb and Lg X-rays. No peaks were found at 8.03 keV and 8.9 keV which were corresponding to K-X-rays of copper (i.e.  $K_{\alpha} = 8.03$  keV,  $K_{\beta} = 8.9$  keV). Target thickness was measured using alpha energy loss method and the thickness of the film was turned out to be  $550\text{mg}/\text{cm}^2$ .



**Fig. 4. Tantalum target on carbon backing (right) and self supporting (left).**

#### **3.4.4 Synthesis of metal polymer nanocomposite for optical applications by atom beam sputtering**

D. K. Avasthi<sup>1</sup>, Y. K. Mishra<sup>1</sup>, D. Kabiraj<sup>1</sup>, N. P. Lalla<sup>2</sup> and J. C. Pivin<sup>3</sup>

<sup>1</sup>Inter University Accelerator Centre, Post Box 10502, New Delhi-110067

<sup>2</sup>UGC-DAE Consortium for Scientific Research, University Campus, Indore

<sup>3</sup>Centre de Spectrometrie Nucleaire et Spectrometrie de Masse, IN2P3-CNRS, Batiment 108, F-91405, Orsay, France

Noble metal particles in insulating (oxides or polymers) matrix, metal polymer NCs and metal insulator multilayers are of wide interest for applications, due to their non-linear optical properties. Apart from the optical applications as band pass filter, there is a tremendous interest in achieving optical absorber extending from visible to far IR region for a variety of applications. The broad absorption band has great potential for applications in the field of solar absorbers. It is of technological importance to achieve the absorption of light over a broad range extending from the visible to infrared region.

The indigenously designed and built atom beam sputtering set up has been used for synthesis of metal polymer NCs. The NCs films were characterized by UV-visible spectrophotometer (Hitachi U3300 and Solid SPEC 3700 SHIMADZU upto 2400 nm), transmission electron microscope (200KV TECNAI G2 20 with LaB6 filament) and Rutherford backscattering spectrometry 2.4 MeV  $\alpha$  particles using ARAMIS the accelerator at CSNSM Orsay. The metal content and film thickness of NCs thin films were analyzed using the RUMP simulation of RBS spectrum and were found to be 30, 55, 71 and 75 atomic % with thicknesses of 52, 54, 89 and 91 nm for the samples a, b, c and d respectively.

The electron diffraction pattern of the NCs sample c is shown in figure 1(a). It reveals the FCC phase of Ag. The nanocomposite nature of the sputtered deposit material is clear by the TEM image in figure 1(b). The TEM image shows that the particles percolate to form aggregates of irregular shapes.

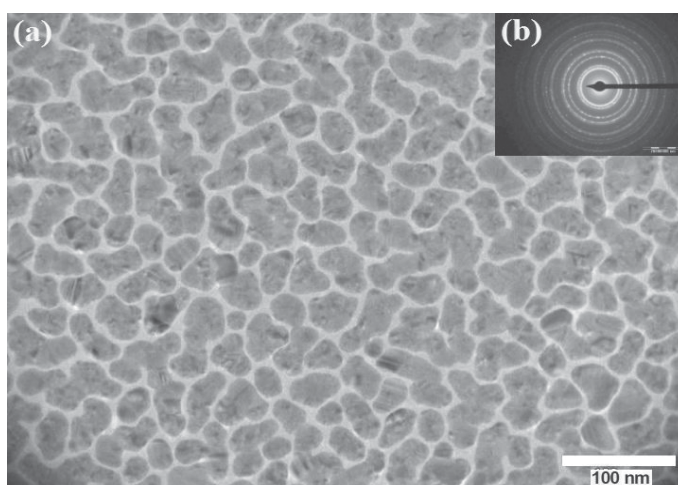


**Fig. 1 (a and b). The TEM micrographs of Ag - PET nanocomposite (c) is shown. The corresponding diffraction rings are shown in the inset. Dark region represents the metal and the light region represents the polymer.**

The transmission and absorption spectra of the prepared samples shown in figure 2 (a) and (b) reveal two interesting features. Firstly, it shows transmission in narrow band around 320 nm, which is wavelength of considerable interest, being the same wavelength as that of HeCd laser. The width of the transmission band varies with the filling factor Ag metal. With the increase in metal volume fraction, the transmission band becomes narrower and the attenuation of transmission intensity at the 320 nm increases. The narrow band results from the superimposition of the absorption spectrum of the sputtered PET polymer (at the lower wavelength region) and that of the Ag nanostructure at the higher wavelength, which is the lower wavelength edge of the broad plasmon resonance of Ag nano structure.

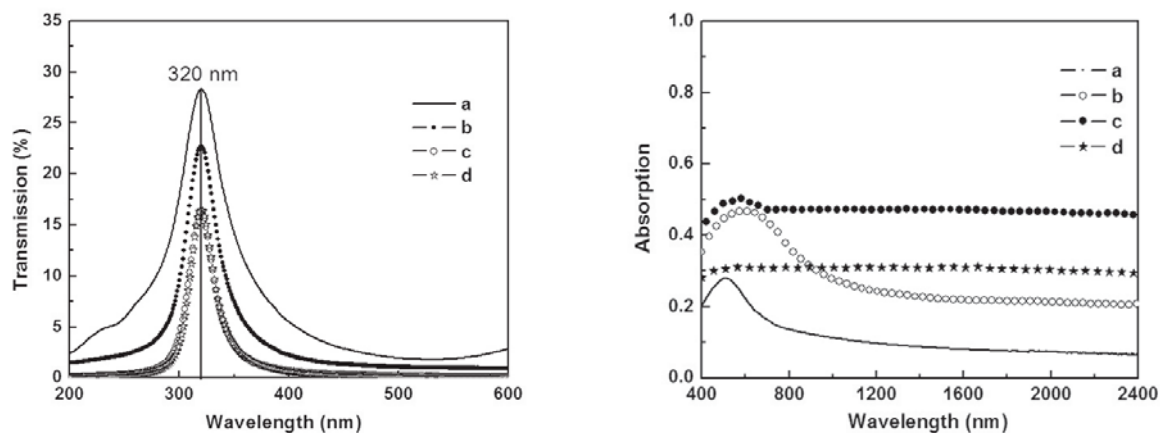


**Fig. 2. (a) The UV-visible transmission spectra for the Ag-PET nano composite (a to d) having different metal volume fractions exhibiting the UV narrow filter characteristics, (b) The optical absorption spectra of Ag-PET nanocomposites (a to d) in visible and in infrared (IR) region, showing the broad absorption extending in IR region.**

Second feature of interest in the UV-visible absorption spectra is the broadband absorption especially for high metal filling fraction (~70 at%). The present results compare well with existing works in the literature.

The broad absorption extending from visible region up to 2400 nm figure 2 (b) is attributed to the three dimensional network of metal nanostructures. High metal particle density results in joining of the two or more metal particles in different orientation in the nanocomposite. Further short-range interactions due to close proximity of nanostructures, like in the present case, also can be responsible for widening of absorption peak.

To conclude, we synthesized [1] 100 nm thin films of Ag-PET nanocomposite of various compositions by a rather new process of atom beam sputtering. These metal polymer nanocomposite films have two specific features suitable for applications as band pass filter at 320 nm and a broadband absorption ranging from 500 nm to far IR region.

## REFERENCE

- [1] D. K. Avasthi, Y. K. Mishra, D. Kabiraj, N. P. Lalla, J. C. Pivin, Nanotechnology 18(2007)125604.

## 3.5 RF & ELECTRONICS LABORATORY

A. Sarkar, S. Venkataramanan, B.K. Sahu, K. Singh, A. Gupta, A. Pandey, P. Singh and B.P. Ajith kumar

### 3.5.1 INGA Clover electronics module production

Production of initial batch of 15 numbers of INGA Clover electronics modules has been initiated. PCBs of various daughter cards have been assembled, individually tested and various sub-assemblies have been prepared. Additional features incorporated in these modules are built-in time delay equaliser, temperature stabilised various control voltages, measurement of cabinet temperature, LED indication of ADC GATE.

### 3.5.2 Pulse shape discrimination (PSD) electronics module for NAND array [1]

At IUAC, we have developed a compact, high density Pulse Shape Discrimination (PSD) electronics module for National Array of Neutron Detectors (NAND). The single width NIM module contains two independent channels of all necessary front end circuits namely shaping amplifier (dynode-energy), CFD, pulse shape amplifier, zero cross discriminator, TAC and TOF Logics. The performances of the module under identical test conditions are compared with commercial electronics setup. After evaluating the prototype of PSD module with neutron detector at IUAC, a initial production of 5 numbers of these module has been done successfully to study the performances. The module has been subjected to thorough off line tests. Some of the features have been shown here. Typical Figure of Merit (FOM) obtained is  $\sim 1.9$  @ 1MeVee LLTH, and typical time resolution obtained is  $\sim 1.2$  nS.

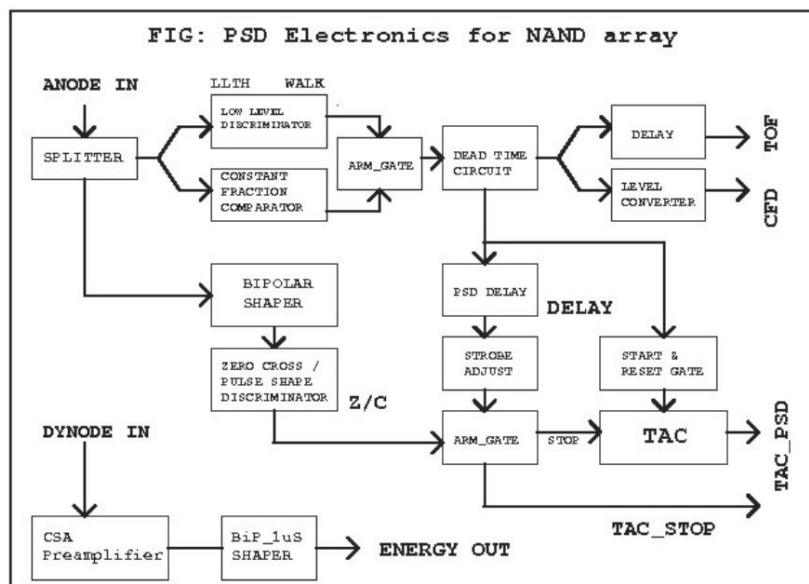


Fig. 1. PSD Electronics for NAND Array

## REFERENCE

- [1] Pulse shape Discriminator for Neutron array at IUAC, Proceeding of DAE symposium on Nuclear Physics, Ref: Vol 51 (2006) Page: 606-607



**Fig. 2. Inside view of Neutron array Electronics module**

### 3.5.3 Development of spare 12 MHz RF power amplifier for multi-harmonic buncher

A spare 12 MHz RF power amplifier has been developed and tested in the Laboratory. It has two stages - the driver stage and the main amplifier stage. The driver stage consisting of two MRF150 MOSFETs in series amplifies the input RF signal and feeds to the final stage. The MOSFETs are capacitively coupled in the driver stage. The output of the driver is taken through an impedance matching transformer.

The final stage is a class AB push-pull/parallel design using MRF150 power MOSFETs. The RF signal from the driver is fed to the input of the MOSFETs through an impedance matching transformer. Each MOSFET is separately biased. Necessary feedback is provided from drain to gate to prevent oscillations. The output from the final stage is taken through a high power impedance matching transformer specially wired using 25-ohm semi-rigid co-axial cable and powdered-iron EE cores. Power supply used for the amplifier is 36V/ 29A SMPS of Cosel make. The DC voltage for the amplifier is set at 28V. Maximum power available is ~ 250 Watts. The amplifier heat sink is water cooled. With RF input of -17 dBm, an output of 100 watts on a 50-ohm load was measured.



**Fig. 3. Inside view of 12MHz RF power amplifier**

### **3.5.4 USB protocol : possibilities and implementation**

The Universal Serial Bus (USB) interface has become extremely popular for commercial as well as research grade instruments, due to its simplicity for end user applications (Plug and lay without restart). For developers, however, USB protocol is very complex and its implementation into their devices has been more complicated when compared to other popular interfaces e.g. LPT1, RS232 etc. In addition there is a need for device drivers as software support on the PC side.

USB protocol implementation into external devices can be done in two ways:

1. By using a micro-controller with "hardware" implemented USB interface.
2. The second option is to use some low-cost micro-controller and to do USB implementation through emulation of USB protocol in the micro-controller "firmware".

The second solution is good for low speed (1.5Mbit/s) USB. It is not recommended for full speed (12Mbit/s) and High speed (480Mbit/s) USB. The first approach using AT43usb355 micro-controller from ATMEL has been tried. The firmware for reading and writing 16 bit serial ADC and DAC has been written. On the PC side PyUSB module has been used for Python language. Operating system is detecting the device as a HID class. The STM interface using this device has been designed.

## **3.6 ELECTRICAL GROUP ACTIVITIES**

U. G. Naik, Raj Kumar

Electrical group has succeeded in keeping its installation uptime to nearly 100% with proper maintenance schedules and monitoring arrangements. This group has also successfully completed the projects and got works envisaged and approved for the financial year 2006-2007.

## **MAINTENANCE:**

### **3.6.1 Captive power arrangement**

Group has managed the emergency power requirements with the available power generating sets and has plans in next plan for bigger sets to meet the demand. One of the helium compressors has always been run on generator supply for every cycle of the plant operation. The group has shown ever readiness in running the systems round the clock and within short notices smoothly.

### **3.6.2 Stabilised power arrangement**

The group has managed to have another year of 100% uptime without a single break in the supply through 1MVA and 500 KVA stabilisers catering to major loads such as A/C plant-II, Helium Compressors and the clean power to IUAC pelletron cum experimental areas.

### **3.6.3 UPS systems**

Electrical group has maintained 50KVA, 3 phase, UPS dedicated to feed motor loads and some computer controls for High Current Injector systems besides a previous base of about 20 nos. of UPS rated from 2-10kVA. Only the 5KVA and above capacity UPS are put on AMC with manufacturer otherwise rest are all maintained by the group. During the present year all UPS were very healthy and had 100% uptime. Routine maintenance was carried out by the manufacturers authorised service centres and the faulty batteries were replaced.

### **3.6.4 Power factor compensation**

Electrical group is very happy to declare that it achieved average power factor almost near to unity throughout the entire year. Our system power factor without correction is about 0.85 and by raising it to near unity we save around Rs.45 lakhs a year from energy billing.

### **3.6.5 Communication equipments**

Electrical group maintains the hand held radio stations (Walkie-talkie) and base station. Till now we have 14nos. of hand held stations and one base station. These are working fine. The group takes the responsibility of getting the revalidation of license periodically from the Ministry of telecommunications.

### **3.6.6 Maintenance of Phase-I & II electrical installations**

The electrical Group is proud to declare here that during this year the installations have performed efficiently and without any breakdowns keeping the uptime at 100%. This was possible to achieve only with dedication and strict maintenance schedules. A few of the major yearly maintenance activities carried out are listed as below.

- Calibration of protection relays.
- Dehydration of transformer oil.
- Air Circuit Breaker servicing- 20 nos.

- Periodic maintenance of LT panels, Distribution boards and other accessories, Lighting, Fixtures, lighting and power circuits.
- Servicing of DG sets 60kVAX2nos, 2X 320 kVA, 1X 100 kVA-twice a year.
- Maintenance of street lighting and earthing.

### **3.6.7 Energy saving**

Energy savings measures taken earlier continued in the areas where we had installed the energy saving time switches and CFL lamps, T-5 lamps etc.

## **PROJECT WORKS:**

### **3.6.8 Installation for beam hall-II**

Power to the experimental areas and both electronics areas made available properly with cables and distribution network.

### **3.6.9 UPS Systems**

Group has made exhaustive study to install centralized UPS for the main lab block and for the new laboratory block. Finalized and procured 2X60 KVA UPS systems to run in parallel redundant mode and installed at the new laboratory block. One more set of same capacity shall be installed in March 2007 for which delivery is in progress. Besides this .to run the Helium Compressors without a break 2x300 KVA UPS systems to run in parallel redundant mode are planned. The order is placed and shall be completed before 31 March 2007.

### **3.6.10 T Power Panels**

Group has planned, designed and placed an order for various kinds of electrical power distribution panels, cables, cable trays and junction boxes at a total order value of more than 40 lakhs. This shall take care of the power input and output of the 2x 300 KVA UPS systems to run in parallel redundant mode.

### **3.6.11 Phase-II part-II installations**

Electrical group has been working in close co-ordination with the CPWD. During the year we have taken over all the installations along with the required documentation.

## **3.7 COMPUTER AND COMMUNICATIONS**

S.Mookerjee, S.Bhatnagar, E.T Subramaniyam

The focus of the group this year was on a major upgrade of the central server pool, and a phased introduction of wireless networking. In addition, the development of software for simulation of ion beams in matter, and the development of data acquisition and analysis software and hardware to support experimental activities in different fields were continued.

### **3.7.1 Central servers**

The central server pool underwent a comprehensive upgrade this year; operating systems on all servers were shifted to Fedora Core 5 from the earlier combination of Red Hat 7.3 and Red Hat 9.0. All central services (mail, web, proxy, firewall, LTS and NIS) were shifted to eight new dual Xeon rack mount servers. Besides saving space and improving manageability, the new servers are faster and have allowed a five-fold increase in user disk space. The mail servers were shifted from qmail/courier IMAP to a Postfix/Dovecot system; this provides a smoother upgrade path in the future, as the qmail system is no longer maintained. Web-based mail interfaces are now available on both the Ernet and Spectranet mail systems. Plotting software QtiPlot was added to the software base on the NIS and LTS servers; this offers users of the Origin package on Windows an upgrade path to Linux. A PXE boot for small data acquisition systems was added to the LTS server; this offers new DAS systems a tested and maintainable boot option. The change of domain to iuac.ernet.in and iuac.res.in was finally completed this year. The bandwidth on the Spectranet link was upgraded to 1.128 Mbps from the earlier 768 Kbps.

The compute cluster was expanded with the addition of ten more nodes to the earlier four. The cluster is now a 20-CPU FC5/LAM-MPI cluster which serves atomic physics, materials science and nuclear physics users.

### **3.7.2 Network infrastructure**

The first wireless networks in the Centre were set up and tested. Wireless coverage now extends to most parts of the main building, to the new Guest House, to the LEIB building and the Engineering building and workshop complex. The network in the LEIB building and the Engineering building was energized this year. The wired LAN in the centre is now based on a fibre gigabit Ethernet backbone, with managed 100 Mb switched connections to more than 450 end nodes. Separate private class C networks were set up to serve the LEIB building, the Engineering building, and wireless users.

### **3.7.3 Software development**

Molecular dynamics simulation code to explore target response to MeV ion beams was further developed as part of a IUAC-CIRIL-LIRIS collaborative effort. Routine upgrades to the administration ERP package were undertaken.

The administration ERP package was upgraded to reflect the purchase order amount instead of the indented amount; this would provide a more accurate and updated snapshot.

### **3.7.4 Data Acquisition System and Hardware development**

A Q-stop functionality was added to the LPCC, and tested in-beam using the LEIBF. A bit pattern functionality was also added to the LPCC, and tested with beam; the CANDLE software was modified accordingly. Twelve LPCC modules were fabricated. Mass production of the ADC modules was started. A new pulse processing design is being explored; ongoing work is aimed at achieving 300 ps time resolution with 42/48 bit time stamping with data on the network. A multi-tier architecture, with a pulse server, store server, process server and client is envisaged.

### **3.8 AIR CONDITIONING, WATER SYSTEM AND COOLING EQUIPMENTS**

P. Gupta, A. J. Malyadri, Bishamber Kumar

#### **Central AC Plant**

IUAC's Central Air Conditioning / Low temperature Cooling System of Phase-1 consisting of 400 TR Central AC plant, performed with 100% uptime. Proper maintenance ensured that the safety record of the plant was maintained at 100% and the power consumption kept at optimum levels. The reciprocating compressors (1,3&4) have logged in approximately 84,000 hours each and new compressor (Comp#2) 8000 hours. Other rotary equipment have logged in about 1,34,500 continuous run hours. The yearly maintenance costs have been maintained at approximately one-eighth the international standards of the installed project cost. The equipment being into their eighteenth year of sustained operations have far outlived their economic lives. In the current year, plenty of repair activities were carried out. This was essential to reset the reliability of the equipment.

The Phase-II, Central AC Plant with a Centrifugal Chiller and with its installed capacity of 250 TR performed to an uptime of 100%. The plant catered to the cryogenic activities and was used extensively for picking up the Phase-I heat loads. This affected a huge energy saving.

The highlight of the operation and maintenance of the above systems was the in-house responsibility and supervision provided to the contracts, thereby affecting substantial savings in the price paid for the operation and maintenance contracts.

Substantial time was devoted by the group to guide CPWD/their contractors for maintenance of proper work quality on the 1x250 TR Screw Chiller based AC system.

#### **Water Systems**

IUAC's centralized water system of phase-I, feeding low temperature cooling water of a total heat removal capacity of 115 TR, potable water supply and the gardening water supply performed to an operational uptime of 100%. This was possible due to the stringent maintenance practices that were followed over the years. The mechanical systems have already overshoot 86,000 hours beyond their expected life span. A strict monitoring on the water quality ensured that the flow paths are in healthy condition. Numerous replacement works were carried out. Several additional equipments were installed.

IUAC's centralized water system of phase-II, feeding low temperature cooling water of a total heat removal capacity of 80 TR, Liquid Helium Cooling water of approx. 350 TR, potable water supply performed to an uptime of 100%. This was possible due to the stringent maintenance practices that were followed over the years. Some replacement works were carried out.

#### **Cooling Equipments**

Availability of these equipment was recorded at around 99%. Several replacements are

being done in a phased manner and several new equipment have been installed.

### **New Construction**

Ph-2 Part-2 Water System was taken over by IUAC on 20-02-2006. However, pending resolution of several defects, the A/C plant could not be taken over by IUAC.

### **3.9 MECHANICAL WORKSHOP**

B.B. Choudhary, Rewa Ram, SK Saini, R Ahuja, Sunder Rao, Jimson Zacharias

The Mechanical Workshop is serving as an in house machining and welding facility for the 15 UD Pelletron accelerator, supporting various laboratories and large number of user community. Workshop has been involved in developmental activities of new systems as well as a large-scale production of beam line components right from the inception of IUAC. This year also most of the beam line components used for the new beam lines were fabricated in the IUAC Workshop. Workshop continues to assist the entire in house fabrication activities of LINAC, RFQ and DTL for HCI, INGA, HYRA, HIRA as well as the Cryogenic component developments.

The major facilities of the workshop are the Machine shop, Weldingshop and the state of art Electron Beam Welding (EBW) machine facility.

The Machine shop is equipped with a five axis Vertical Machining Centre and a CNC lathe. Four conventional lathes, two milling machines and radial drilling machine cater the tool room jobs. Most of these machines are of HMT make, fitted with DRO's for achieving higher accuracy and better productivity. Apart from these, we have cylindrical grinder, tool and cutter grinder, horizontal and vertical band saw machines, sand blasting machine etc for general requirement. We also have the CAD facility, Solid Works for the design and the drafting purposes. We also have VISI CAM for the CAM support for the Vertical Machining Centre.

Welding -shop is having high quality TIG welding machines and equipment. Some of the TIG machines can give pulsed arc for the thin section welding. Air plasma cutter with a capacity to cut up to 40mm thickness of stainless steel is used extensively. Aluminum welding and Oxy-acetylene cutting and brazing set ups are also available. We have a micro -plasma machine from Air Liquide, France for very thin section welding.

The Electron Beam Welding facility is fully operational and fabrications of fifteen resonators are in full swing.

University Grants Commission Chairman inaugurated the new workshop building in presence of honorable guests and IUAC Director on August 14th 2006. Now the new building houses all the machine shop, welding shop and other engineering services

All the machines, mentioned above, are working in good conditions, because of timely maintenance and careful handling. Apart from the people engaged in the workshop, other academic personnel and students are also capable of handling the machines.

IUAC workshop is providing apprentice training for the ITI passed students in both welding shop as well as in machine shop. Basic workshop training is provided for the scientist trainees and Ph.D. students enrolled in IUAC.

### 3.10 HEALTH PHYSICS

S.P.Lochab, R.G. Sonkawade and Birender Singh

As radiation physics has emerged over the years as a separate discipline of research and development activities, increasing use of particle accelerators of various types have opened up new avenues for research in this field. Health physics involves in the field of radiation research, development and safety aspects. The radiation safety status of Pelletron accelerator in IUAC as per AERB regulation is maintained. On line and off line research support to the users is provided i.e. Radiation survey, Personnel monitoring etc.

Newly developed TLD phosphors were studied for ion beam dosimetry purpose using 48MeV  ${}^7\text{Li}$ , 100MeV  ${}^{16}\text{O}$  and 200MeV  ${}^{107}\text{Ag}$  ions beam in Mat. Sc. beam line. Door Interlocks for Mat. Sc.-II and Vault-II are completed. Development of new shielding materials for gamma and neutron radiation, developments of new thermoluminescence materials for radiation dosimetry and environmental radiation monitoring are taken up apart from day to day activities. The remote readings of gamma and neutrons installed in BH-II are brought in the control room and tested with gamma and neutron sources.

Currently health physics group is actively involved with different universities on various aspects of radiation research.

#### 3.10.1 Development and study of new TLD phosphors

Nano and micro particles of  $\text{CaS}:\text{Bi}$ ,  $\text{CaSO}_4:\text{Eu}$ ,  $\text{Ca}_{0.03}\text{Ba}_{0.97}\text{SO}_4:\text{Eu}$ , and nano particles of  $\text{MgB}_4\text{O}_7:\text{Dy}$  were prepared and studied for their TL properties. Different types of TLD-materials were exposed to  ${}^7\text{Li}$  (24MeV and 48MeV), 100MeV  ${}^{17}\text{O}$  and 200MeV  ${}^{107}\text{Ag}$  ions in the fluence range of  $1 \times 10^9 - 5 \times 10^{13}$  and thermoluminescence, photoluminescence, structural modifications, UV absorption, ESR studies were carried out.

##### (i) Study of $\text{CaS}:\text{Bi}$ nanocrystalline phosphors for thermally stimulated phenomena

S P Lochab<sup>1</sup>, Vinay Kumar<sup>2</sup>, Ravi Kumar<sup>1</sup> and Nafa Singh<sup>2</sup>

<sup>1</sup>Inter University Accelerator Center, New Delhi-110067

<sup>2</sup>Department of Physics, Kurukshetra University, Kurukshetra-136 119

The thermoluminescence (TL) studies of  $\text{CaS}:\text{Bi}$  nanocrystalline phosphors prepared by the wet chemical co-precipitation method and exposed to  $\gamma$ -rays have been discussed. The average grain size of the samples was estimated as 35 nm using Scherrer's formula. The samples exhibit a complex TL glow curve with multiple peaks. Sample exposed to  $\gamma$  rays showed that the TL

intensity increases linearly as the radiation doses increased in the 1.012-40.48 mGy range. The trap parameters namely, activation energy (E), order of kinetics (b) and frequency factor (s) of the main peaks of the CaS:Bi(0.08 mole%) sample have been determined using Chen's method. The effect of different dopant concentrations and different heating rates has also been discussed.

**(ii) Thermoluminescence and Photoluminescence Study of nanocrystalline Ba<sub>0.97</sub>Ca<sub>0.03</sub>SO<sub>4</sub>:Eu phosphor**

S.P. Lochab<sup>1</sup>, P D Sahare<sup>2,\*</sup>, R S Chauhan<sup>3</sup>, Numan Salah<sup>2</sup>, Ranju Ranjan<sup>2</sup> and A. Pandey<sup>4</sup>

<sup>1</sup>Nuclear Science Centre, New Delhi-110067

<sup>2</sup>Department of Physics & Astrophysics, University of Delhi, Delhi-110007

<sup>3</sup>Department of Physics, R.B.S. College, Dr. B.R. Ambedkar Univ., Agra

<sup>4</sup>Department of Physics, Sri Venkateswara College, University of Delhi

\* Department of Physics, University of Pune, Pune, Maharashtra.

Nanocrystalline Ba<sub>0.97</sub>Ca<sub>0.03</sub>SO<sub>4</sub>:Eu having grain size 55 nm has been prepared and a comparative study has been carried out with its corresponding microcrystalline form. The TL glow curve of the nanophosphor has a prominent peak at 161°C and a very small hump at 225°C. The TL sensitivity of the nanophosphor is about 0.1 times that of the microphosphor. Orders of kinetics of the TL peaks of the nanophosphor are worked out and are compared with those of the microphosphor. PL emission spectra of the nano and the micro phosphors are studied and their results are correlated with the other experimental findings. The TL response of the nanophosphor is linear in the dose range of 1 Gy to 20 KGy which is much wider than that of its corresponding microcrystalline form. The glow curve shape and structure also do not change in the linear dose range and since the TL response is linear at higher doses the nanophosphor is quite well suited for high dose measurements.

**(iii) Nanocrystalline MgB<sub>4</sub>O<sub>7</sub>:Dy for High Dose Measurement of Gamma Radiation**

S.P. Lochab<sup>1</sup>, P D Sahare<sup>2,\*</sup>, R S Chauhan<sup>3</sup>, Numan Salah<sup>2</sup>, Ranju Ranjan<sup>2</sup> and A. Pandey<sup>4</sup>

<sup>1</sup>Nuclear Science Centre, New Delhi-110067

<sup>2</sup>Department of Physics & Astrophysics, University of Delhi, Delhi-110007

<sup>3</sup>Department of Physics, R.B.S. College, Dr. B.R. Ambedkar Univ., Agra

<sup>4</sup>Department of Physics, Sri Venkateswara College, University of Delhi

\*Department of Physics, University of Pune, Pune, Maharashtra.

Magnesium borate activated by dysprosium (MgB<sub>4</sub>O<sub>7</sub>:Dy) is a low-Zeff, tissue-equivalent material that is commonly used for medical dosimetry of ionizing radiations such as gamma and x rays using the thermoluminescence (TL) technique. Nanocrystals of the same material are produced and their TL characteristics are studied. It is found that the nanocrystalline MgB<sub>4</sub>O<sub>7</sub>:Dy with a dopant concentration of 1000 ppm is the most sensitive amongst varying dopant concentra-

tions, with its sensitivity equal to 0.025 times that of the standard phosphor  $\text{CaSO}_4:\text{Dy}$ . The glow curve has two peaks at  $154^\circ\text{C}$  and  $221^\circ\text{C}$ . The nanophosphor has very poor sensitivity for low doses up to 10 Gy but beyond this dose the phosphor exhibits a linear response up to 5000 Gy. On increasing the dose further the response first becomes supralinear and then sublinear, finally resulting into saturation. Considering also its low fading particularly under post-irradiation annealing and excellent reusability features, this nanophosphor may be used for high dose (10-5000 Gy) measurements of ionizing radiations.

**(iv) TL characteristics of  $\text{Ba}_{0.97}\text{Ca}_{0.03}\text{SO}_4:\text{Eu}$  by  $^7\text{Li}$  ion beam**

S.P. Lochab<sup>1</sup>, P.D Sahare<sup>2</sup>, R.S. Chauhan<sup>3</sup>, Numan Salah<sup>2</sup>, Ranju Ranjan<sup>2</sup>

<sup>1</sup>Inter-university Accelerator Centre, New Delhi-110067

<sup>2</sup>Department of Physics & Astrophysics, University Of Delhi

<sup>3</sup>Department of Physics, RBS College, Agra-282002

Thermoluminescence (TL) of  $\text{Ba}_{0.97}\text{Ca}_{0.03}\text{SO}_4:\text{Eu}$  phosphor, irradiated with 48 MeV  $^7\text{Li}$  ions at different fluences in the range  $1 \times 10^9$ - $1 \times 10^{12}$  ions/cm<sup>2</sup>, has been studied. The phosphor was prepared by the chemical co-precipitation technique. The samples from the same batch were also irradiated with g-rays from a  $\text{Cs}^{137}$  source for comparative studies. It has been found that the TL glow peak at 460 K, seen prominently in g-irradiated sample, appeared as a small shoulder at around 465 K in  $^7\text{Li}^{3+}$  ion irradiated sample, while that observed as a shoulder in the former at 430 K, dominantly appeared in the latter at around 435 K. Trapping parameters of both, ion beam and g-irradiated materials, were also obtained after the deconvolution of the glow curves. The TL response curve of the ion beam irradiated samples has a linear ion beam fluence response over the range  $1 \times 10^9$ - $1 \times 10^{10}$  ions/cm<sup>2</sup>. This property along with its low fading and simple glow curve structure makes  $\text{Ba}_{0.97}\text{Ca}_{0.03}\text{SO}_4:\text{Eu}$  phosphor a suitable dosimeter for heavy charged particles (HCP).

**(v) Structural modification and photo-luminescence in  $\text{CaS}:\text{Bi}$  nanophosphors induced by SHI**

Vinay Kumar<sup>1</sup>, Nafa Singh<sup>1</sup>, Ravi Kumar<sup>2</sup> and S P Lochab<sup>2</sup>

<sup>1</sup>Department of Physics, Kurukshetra University, Kurukshetra-136 119

<sup>2</sup>Inter University Accelerator Center, New Delhi - 110067

$\text{CaS}:\text{Bi}$  nanocrystalline powder of average grain size 35 nm was prepared by wet chemical co-precipitation method and irradiated with 100 MeV oxygen ions at fluences between  $1 \times 10^{12}$  and  $1 \times 10^{13}$  ion/cm<sup>2</sup>. The irradiation induced damage and modifications were studied using X-ray Diffraction (XRD), transmission electron microscopy (TEM) and photoluminescence (PL) spectroscopy. With the increase in ion fluences, the crystallinity of  $\text{CaS}$  was destroyed upto 25.9 % for the reflection (200) and 21.1 % for the reflection (220) and the peaks broadens at a much faster rate due to grain breaking process. Structural parameters such as grain size, strain and dislocation density have shown a significant change after ion irradiation. The effects of different dopant concentrations on PL emission intensity after irradiation were also investigated. A blue shift of the

photoluminescence peak with increasing ion fluence was noticed and was also ascribed to a decrease in the CaS grain size.

**(vi)  $K_3Na(SO_4)_2$ :Eu nanoparticles for high dose of ionizing radiation**

P D Sahare<sup>1, \*</sup>, Ranju Ranjan<sup>1</sup>, Numan Salah<sup>2</sup> and S P Lochab<sup>3</sup>

<sup>1</sup>Department of Physics & Astrophysics, University of Delhi, Delhi-110007

<sup>2</sup>Dept. of Physics, Faculty of Applied Sciences, Thamar University, Yemen

<sup>3</sup>Inter-University Accelerator Centre, New Delhi-110067

\* Department of Physics, University of Pune, Pune, Maharashtra.

$K_3Na(SO_4)_2$ :Eu nanocrystalline powder was synthesized by the chemical co-precipitation method. The x-ray diffraction pattern of the nanomaterials shows a hexagonal structure for its crystals having grain size of 28 nm. Transmission electron microscopy revealed that the  $K_3Na(SO_4)_2$ :Eu nanoparticles are single crystals with almost a uniform shape and size. Thermoluminescence (TL) was taken after irradiating the samples at various exposures of g-rays from a <sup>60</sup>Co source. A prominent TL glow peak is observed at 423K along with three small peaks/shoulders at around 382, 460 and 509 K. The observed TL sensitivity of the prepared nanocrystalline powder is around 4 times more than that of LiF : Mg,Ti (TLD-100) phosphor. The 423K peak of the nanomaterial phosphor eventually shows a near linear response with exposures increasing up to very high values (as high as 70 kGy), where all the other TLD phosphors saturate. This property along with its other desired properties such as high sensitivity, relatively simple glow curve structure and low fading makes the nanocrystalline phosphor a suitable dosimeter to estimate low as well as high exposures of g-rays. TL analysis using the glow curve deconvolution technique was also done for determining different trapping parameters.

**(vii) Effect of swift heavy ion irradiation on optical properties of nanocrystalline CaS:Bi phosphors**

Vinay Kumar<sup>1</sup>, Nafa Singh<sup>1</sup>, Ravi Kumar<sup>2</sup> and S P Lochab<sup>2</sup>

<sup>1</sup>Department of Physics, Kurukshetra University, Kurukshetra-136 119

<sup>2</sup>Inter University Accelerator Center, New Delhi-110067

Luminescence studies of CaS:Bi nanocrystalline phosphors synthesized by wet chemical co-precipitation method and irradiated with swift heavy ions ( $Ag^{+15}$ -ion with 200MeV) have been carried out. The samples have been irradiated at different ion fluences in the range  $1 \times 10^{12}$ - $1 \times 10^{13}$  ions/cm<sup>2</sup>. The average grain size of the samples before irradiation was estimated as 35 nm using line broadening of XRD (X-ray diffraction) peaks and TEM (transmission electron microscope) studies. The blue emission band of nanosized CaS:Bi<sup>3+</sup> at 401nm is from the transition of  $3P_1 \rightarrow 1S_0$  of the Bi<sup>3+</sup>. After ion irradiation the lattice constant (a) decreases and optical energy band gap increased which may be due to irradiation induced grain fragmentation. We have studied the optical and luminescent behavior of the samples by changing the ion energy. It has been observed that ion irradiation enhanced the luminescence properties of samples.

### **(viii) Synthesis and characterization of CaS:Bi nanocrystallites phosphors**

Vinay Kumar<sup>1</sup>, Nafa Singh<sup>1</sup>, Ravi Kumar<sup>2</sup> and S P Lochab<sup>2</sup>

<sup>1</sup>Department of Physics, Kurukshetra University, Kurukshetra-136 119

<sup>2</sup>Inter University Accelerator Center, New Delhi-110067, India

Nanosized bismuth doped calcium sulfide (CaS:Bi) particles have been synthesized by a wet chemical co-precipitation method. The average size of the nanoparticles was found to be about 30 nm. The particles were characterized by x-ray diffraction (XRD), transmission electron microscopy (TEM), UV- vis spectroscopy and fluorescence spectroscopy. The effect of particle size on the photoluminescence (PL) of CaS:Bi has been studied. The optimum dopant concentration was found to be 0.025 mol% of bismuth for maximum PL emission intensity. A comparative study between bulk CaS:Bi prepared by a reduction method and nanosized CaS:Bi made by the wet co-precipitation method has been carried out. Increase in band gap with decrease in particle size has been explained on the basis of the quantum size effect. The PL intensity of the nanoparticles was found to increase to almost twice that of the bulk particles. The effect of different dopant concentrations on emission intensity has also been studied

### **(ix) UV-dosimetric properties of bismuth doped CaS nanocrystalline phosphor**

Vinay Kumar<sup>1</sup>, Nafa Singh<sup>1</sup>, Ravi Kumar<sup>2</sup> and S P Lochab<sup>2</sup>

<sup>1</sup>Department of Physics, Kurukshetra University, Kurukshetra-136 119

<sup>2</sup>Inter University Accelerator Center, New Delhi-110067

The irradiation effect on bismuth doped CaS nanocrystalline phosphors and their possible applications to solid state dosimetry have been studied. The wet chemical co-precipitation method has been used for preparation of nanocrystallites. In UV exposed CaS nanocrystallites, the thermoluminescence glow curve consists of two peaks at 439 and 561 K. The effect of different concentrations, dose dependence, fading and reusability in CaS:Bi nanocrystallites have been investigated. The high temperature peak (dosimetric peak) intensity is nearly linear in a wide range of UV exposure. It can be concluded from the results that the TL glow curve shifts to higher temperature in nanocrystalline phosphors. The samples have been found to have excellent reusability. The strong peak at 561K of CaS:Bi (0.08 mol%) is well above the room temperature. Therefore, the thermal fading during storage at room temperature is not expected to occur. Under suitable condition, this peak may have a potential for the UV dosimetric application, using TL techniques. A blue shift in the PL intensity has been found, which may be attributed to the quantum size effect.

## **3.11 CIVIL WORKS**

M.K.Gupta and Manohar Lal Chandel

Civil section is associated with the following activities:

- (i) **Major expansion Project ( right now Phase II - Part II expansion)**
- (ii) **Minor Projects**
- (iii) **Minor Works** (additions, alterations, renovation in the existing Civil works)
- (iv) **Civil Maintenance**
- (v) **External Cleaning of the Campus**
- (vi) **Liason** with various Govt. and outside agencies for statutory approvals and various civic problems
- (vii) **Important Civil Activities during the Year 2006-07**

Following important civil works were undertaken during the year 2006-07 in addition to routine civil maintenance and minor works:

- Complete handing over of Phase II-Part II (Stage 1)project to IUAC by CPWD
- Construction of Beam Hall-III in progress by CPWD
- Ceramic tile flooring in toilets of Phase II housing
- PVC partitions in Engineering building and in R.N. 101,225 &106 of Main Lab. Building
- Venetian blinds in LEIB building and Engineering building
- Fibreglass sheet covering in corridor outside Beam Hall-II
- Wiremesh doors in Sumeru-III blocks
- Phase II housing internal painting
- Construction of labour toilet near temporary structures
- Antitermite treatment in new Guest house
- Antitermite treatment in Sumeru-III blocks

### **3.12 COMPRESSED AIR SYSTEM AND MATERIAL HANDLING EQUIPMENTS**

K.K. Soni and Bishamber Kumar

This section was associated with the following activities:

i) Compressed Air System: Compressed air plant ( Ph-I & PH-II ) consisting of two nos. reciprocating compressors each of 60 M<sup>3</sup>/Hr and two nos. screw compressors each of 115 M<sup>3</sup>/Hr capacity, air dryers & filters with capacity of 3000 lpm @ 9.00 Kg/cm<sup>2</sup> have been

maintaining uninterrupted air supply to tower, Beam Hall- I, Beam Hall -II buildings, round the clock. In order to further increase the reliability of the Compressed air supply at constant pressure, a 25 M3 Storage tank is designed and is under fabrication. It will be installed in the Compressed air line .Pneumatic connections have been extended to all the labs. Further to ensure dew point of the air, the compressed air is passed through two refrigerated type air dryers of 4300 LPM capacity. Ultra high filters of boro silicate and carbon filters are provided in different location of the compressed air to provide clean air free from dust and oil particles. Since Reciprocating compressors which are more power consuming and source of excess oil contamination in the compressed air, therefore, two reciprocating compressors are replaced by one Screw Air Compressor of 2208 lpm capacity. Compressed air piping has been extended to Lab I, Lab II and New Workshop building. An additional GA-15 air compressor is being added to the system to meet the increased requirement of compressed air and also to make the system more reliable.

ii) Industrial Gases: Various industrial gases required in different labs have been made available from time to time. Special gases like Iso Butane and mixture gases are also procured for labs.

iii) Elevator: Elevator has been running smoothly and monthly preventive maintenance of the same is carried out to minimise the operational break down.

iv) Material Handling System : Periodic maintenance / servicing of more then 10 E.O.T cranes and electric hoists of various capacity varying from 1 Tonne to 7.5 Tones are being carried out periodically and the same have been working smoothly. Two more cranes of 2 Tone capacities are installed in EBWM room and Material Storage area. A 2 Tones EOT Crane has been installed in new workshop building to handle the heavy items during machining of parts and also during maintenance of Machines. All the cranes are put on remote control operation for safe handling of machines.

v) Fire Extinguishers: Annual refilling and periodic maintenance of all the fire extinguishers have been carried out. New fire extinguishers have been installed in newly constructed BH II store area , Lab I and Lab II area, Workshop building. Some more signal including the "Escape route" in emergency is added in the building with GLOW LIGHT which shines even in darkness .Demonstration for use of Fire extinguishers have been arranged and all the users and IUAC employees are trained to use the fire extinguishers.

### **3.13 DATA SUPPORT LABORATORY**

V.V.V. Satyanarayana, R. Ruby Santhi and P. Sugathan

Data Support Laboratory provides user support to various experimental groups setting up NIM & CAMAC modules for data acquisition during experiments. Data room is providing two independent On-line data acquisition systems for data collection during experiments. Apart from providing regular user support & maintenance of the setup, we have developed a few electronic modules and serviced a number of NIM & CAMAC modules. The lab had procured new modules, cables & connectors for data acquisition purpose.



**Fig.1. View of the Data room setup at IUAC**

### **3.13.1 Data Acquisition Tester Module**

A single width NIM module to test the basic function of the Data acquisition system has been designed and fabricated. This module gives a fixed 2 volts amplitude Gaussian pulse of  $1\mu\text{s}$  shaping time at a repetition rate of 1 kHz. The module also gives TTL and NIM strobes of  $10\mu\text{s}$  width to gate Peak sensing ADCs used in Data acquisition systems.

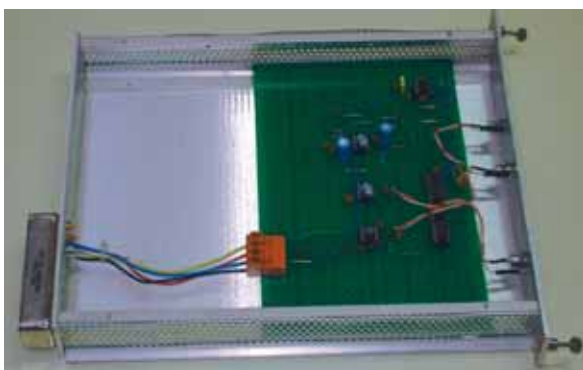


**Fig. 2a Inside view**



**Fig. 2b Front view**

### **3.13.2 Gate and Delay Generator module**

A single width NIM module to generate gate pulses to ADCs in Data acquisition systems is fabricated and tested. It accepts either polarity of logic pulses, provides an adjusted delay for each input pulse, and generates output pulses with both polarities that have an adjusted amplitude and width. It serves as a convenient interface between logic pulse origin and its end use. The logic pulse delay is adjustable from  $0.1\mu\text{s}$  through  $110\mu\text{s}$  in three overlapping ranges. The amplitudes of both polarities of output pulses are adjustable within the range of 2 to 10V. The output pulse

width can be adjusted within the range of 400ns through 17  $\mu$ S in two overlapping ranges.

### 3.13.3 FPGA based 13 bit Sliding Scale CAMAC ADC

This is a single channel 13 bit peak sensing Analog to digital converter module to measure unipolar signals from shaper amplifiers in the range of 0 to 5V. This module is made by adding sliding scale technique to the 12 bit CAMAC adc made in the year 2002-2003. This is a single width CAMAC module using AD676 Successive approximation type analog to digital converter from Analog Devices, and the logic part of the circuit is integrated into a single XC4010EPQ160 Xilinx FPGA using VHDL design.

### 3.13.4 FPGA based 8K ADC with Histogram generator

FPGA based Histogram generator along with Peak sensing circuit and Analog to Digital Converter is wired on a single board with an interface to the PC using ISA bus. The peak sensing circuit detects the height of the input and is given to an analog to digital converter based on the integrated chip AD676 from Analog Devices. A threshold comparator sitting at the input initiates the conversion process and after the conversion complete data will be given to the histogram generator implemented using Xilinx XC4010EPQ160 FPGA using VHDL design. •



**Fig. 3. FPGA based 8K ADC with Histogram generator**

### 3.13.5 Multi Channel Analyzer using Embedded PC

A portable Multi Channel Analyzer (MCA) system has been developed using locally available 12 bit ADC board attached to an embedded PC system. The MCA input accept 0-5V unipolar Gaussian pulses from any standard spectroscopy amplifiers and converts it into a 12-bit digital output using the ADC (AD676 Successive Approximation Register type). The on-line data acquisition is accomplished by parallel port data transfer using "mca" software developed at IUAC. The software is installed in an Embedded PC (Vortex86TM from ICOP Technology) with 512MB disk capacity. This MCA was made in the year 2005. Two more numbers are made this year.

### 3.13.6 Servicing and Maintenance

A few numbers of NIM and CAMAC modules were serviced and repaired. The following items are serviced during the year

- 1) NIM Bin power supply, EG&G Ortec model 4001C
- 2) Pre-amplifier, Nuclear Enterprises model NE5289
- 3) Timing Filter Amplifier, EG&G Ortec model 474
- 4) 24 bit Histogram generator, IUAC make
- 5) CAMAC Crate controller, IUAC make

Following Electronic module are added to data acquisition resource pool

- 1) Tektronix make 350MHz, 2.5GS/s Digital Phosphor Oscilloscope
- 2) Canberra 2003BT Pre-amplifiers
- 3) CAMAC power supplies
- 4) SHV, BNC and Lemo connectors and Cables